

Table S1. NAD precursor availability in DMEM, mouse chow, the serum of mice, and circulatory turnover fluxes (F_{circ}). Related to Figure 1, Figure 5 and STAR Methods. DMEM and chow data are from the manufacturer. Serum data are LC-MS measurements made here (mean \pm s.d., $n = 3$). Turnover fluxes were calculated from infusion rate and steady state labeling percentage (Hui *et al.*, 2017) (mean \pm s.d., $n = 3$).

	Concentrations			Turnover fluxes
	DMEM	Mouse chow	Mouse serum	F_{circ}
Trp	80 μ M	13.7 mM	46 \pm 4 μ M	2.8 \pm 0.4 nmol/g/min
NAM	32 μ M	-	2.1 \pm 0.2 μ M	0.55 \pm 0.04 nmol/g/min
NA	-	0.98 mM	0.22 \pm 0.07 μ M	2.0 \pm 0.9 pmol/g/min
NMN	-	-	1nM	-
NAD	-	-	< 1nM	-
NR	-	-	7.0 \pm 2.3 nM	-

Table S2. NAD fluxes and protein PARylation across five human breast cancer cell lines. Related to Figure 3. Data for lysate PARylation (detected as described (Krukenberg *et al.*, 2014)) are mean \pm s.d., $n = 6$. Data for NAD concentration are mean \pm s.d., $n = 3$. Data for labeling $t_{1/2}$ and PARP-mediated consumption are mean \pm 95% confidence interval (L.B. lower boundary, U.B. upper boundary).

	KPL1	MCF7	AU565	T47D	SKBR3	
Lysate PARylation (ug PAR per mg protein)	61 \pm 10	39 \pm 8	2.9 \pm 0.7	2.1 \pm 0.6	1.4 \pm 0.5	
NAD pool (nmol per million cells)	2.1 \pm 0.3	4.0 \pm 0.2	4.3 \pm 0.2	1.9 \pm 0.2	2.6 \pm 0.4	
NAD labeling $t_{1/2}$ (h)	12.2 \pm 0.7	13.5 \pm 0.4	9.7 \pm 0.5	8.6 \pm 0.3	9.9 \pm 0.5	
NAD consumption by PARP (pmol per million cells per h)	Best	17	53	56	38	48
	L.B.	14	46	44	28	38
	U.B.	25	55	60	43	55

Table S3. Half-time for NAD labeling by ^2H -NAM and for NAD depletion upon adding FK866 (100 nM) in different cell lines. Related to Figure 4. Data are mean \pm 95% confidence interval.

hour	Breast Cancer				GI Cancer				Melanoma		Differentiation	
	MDA-MB-231	MDA-MB-468	MCF7	T47D	HCT116	HepG2	Panc1	8988T	SK-MEL-2	SK-MEL-28	C2C12	3T3-L1
NAD labeling half-life	7.1 \pm 1.2	5.6 \pm 0.4	13.2 \pm 0.3	8.5 \pm 0.6	6.6 \pm 0.6	8.1 \pm 0.3	12.3 \pm 2.5	10.2 \pm 0.4	12.9 \pm 0.5	7.3 \pm 0.8	8.3 \pm 1.2	5.1 \pm 0.3
Time to deplete half NAD	7.3 \pm 0.3	4.9 \pm 0.3	13.2 \pm 0.9	6.4 \pm 0.2	7.1 \pm 0.9	7.3 \pm 0.7	11.9 \pm 1.0	7.4 \pm 0.6	11.2 \pm 1.0	7.9 \pm 1.4	8.3 \pm 0.8	5.9 \pm 0.6

Table S4. Concentrations of NAM, NAD(H), and NADP(H) in murine tissues. Related to Figure 5 and STAR Methods. Data are mean \pm s.d., $n = 4$.

μ M	White Adipose	Brain	Heart	Kidney	Liver	Lung	Pancreas	Skeletal Muscle	Small Intestine	Spleen
NAM	8 \pm 3	46 \pm 13	60 \pm 22	58 \pm 12	44 \pm 18	51 \pm 24	40 \pm 17	47 \pm 13	90 \pm 13	64 \pm 10
NAD(H)	35 \pm 9	258 \pm 53	459 \pm 47	518 \pm 42	690 \pm 48	146 \pm 21	467 \pm 59	219 \pm 53	241 \pm 43	255 \pm 35
NADP(H)	2.5 \pm 0.2	55 \pm 21	32 \pm 5	90 \pm 33	97 \pm 20	63 \pm 31	24 \pm 8	101 \pm 40	53 \pm 26	49 \pm 19

Table S5. Metabolic flux distributions (normalized to weight) with confidence intervals and SSR in tissues. Related to Figure 6. Fluxes are normalized to weight. The goodness of fit was evaluated by chi-square test, $\chi^2_{0.05}(df=15)=25$. Each flux is shown with 95% confidence intervals of NAD labeling half-lives (L.B. lower boundary, U.B. upper boundary).

Tissue		Flux ($\mu\text{M} / \text{h}$)				Half-life (h)	SSR
		f_1	f_2	f_3	f_4		
White Adipose	Best	0.0	0.1	2.3	10.7	2.3	38.2
	L.B.	0.0	0.1	2.3	8.1	3.0	
	U.B.	0.0	0.1	2.2	14.9	1.6	
Brain	Flux	0.0	0.1	17.1	46.0	3.9	20.6
	L.B.	0.0	0.1	17.0	37.4	4.8	
	U.B.	0.0	0.1	17.0	57.4	3.1	
Heart	Flux	0.0	1.0	21.0	120.5	2.6	21.6
	L.B.	0.0	1.0	20.7	90.5	3.5	
	U.B.	0.1	1.1	20.7	169.5	1.9	
Kidney	Flux	6.3	5.4	55.7	124.0	2.6	23.4
	L.B.	6.1	5.2	55.9	105.0	3.1	
	U.B.	6.6	5.5	54.8	148.0	2.2	
Lung	Flux	0.0	0.8	37.4	41.9	2.4	153.0
	L.B.	0.0	0.7	39.2	36.9	2.7	
	U.B.	0.0	0.8	35.7	47.7	2.1	
Skeletal Muscle	Flux	0.0	0.0	9.4	10.4	14.6	19.8
	L.B.	0.0	0.0	8.4	6.5	23.2	
	U.B.	0.0	0.0	10.1	14.7	10.3	
Pancreas	Flux	0.0	3.5	52.1	38.1	7.8	66.2
	L.B.	0.0	3.3	49.4	32.5	9.1	
	U.B.	0.0	3.7	54.1	44.3	6.8	
Small Intestine	Flux	0.0	1.2	73.6	581.6	0.3	99.3
	L.B.	0.0	1.1	76.1	435.6	0.4	
	U.B.	0.0	1.2	71.0	859.6	0.2	
Spleen	Flux	0.0	1.1	69.4	409.2	0.4	53.5
	L.B.	0.0	1.0	71.7	325.2	0.5	
	U.B.	0.0	1.1	67.0	547.2	0.3	
Liver	Flux	55.0	0.9	54.0	176.4	2.1	16.1
	L.B.	54.2	0.8	54.5	140.4	2.4	
	U.B.	55.7	1.0	52.1	228.4	1.7	

Table S6. Measured and model-predicted NAD and NAM labeling fractions in tissues, from co-infusion of [U-¹³C]Trp and [2,4,5,6-²H]NAM (20:1 ratio, equal to their physiological ratio in serum) for 5 h. Related to Figure 6. Correlation coefficient is 0.993. Measured data are mean ± s.d., n=3.

Tissue	Isotopic fraction	Simulated	Measured		Tissue	Isotopic fraction	Simulated	Measured	
			Mean	s.d.				Mean	s.d.
White Adipose	NAM M+0	0.894	0.849	0.010	Skeletal Muscle	NAM_0	0.853	0.724	0.012
	NAM M+3	0.044	0.078	0.009		NAM M+3	0.018	0.044	0.013
	NAM M+4	0.055	0.068	0.002		NAM M+4	0.118	0.220	0.011
	NAM M+6	0.007	0.006	0.002		NAM M+6	0.010	0.012	0.011
	NAD M+0	0.945	0.940	0.000		NAD M+0	0.983	0.987	0.009
	NAD M+3	0.051	0.059	0.007		NAD M+3	0.016	0.013	0.005
	NAD M+6	0.003	0.002	0.006		NAD M+6	0.001	0.000	0.014
Brain	NAM M+0	0.866	0.792	0.012	Pancreas	NAM M+0	0.757	0.764	0.010
	NAM M+3	0.040	0.046	0.009		NAM M+3	0.048	0.058	0.002
	NAM M+4	0.084	0.151	0.003		NAM M+4	0.176	0.139	0.008
	NAM M+6	0.010	0.011	0.000		NAM M+6	0.019	0.040	0.000
	NAD M+0	0.950	0.975	0.000		NAD M+0	0.946	0.949	0.000
	NAD M+3	0.047	0.025	0.001		NAD M+3	0.051	0.049	0.001
	NAD M+6	0.003	0.000	0.001		NAD M+6	0.003	0.002	0.000
Heart	NAM M+0	0.908	0.896	0.006	Small Intestine	NAM M+0	0.780	0.786	0.005
	NAM M+3	0.039	0.033	0.011		NAM M+3	0.169	0.159	0.012
	NAM M+4	0.047	0.064	0.005		NAM M+4	0.036	0.054	0.006
	NAM M+6	0.007	0.006	0.000		NAM M+6	0.015	0.012	0.001
	NAD M+0	0.956	0.975	0.012		NAD M+0	0.798	0.874	0.013
	NAD M+3	0.042	0.024	0.012		NAD M+3	0.189	0.120	0.013
	NAD M+6	0.003	0.001	0.001		NAD M+6	0.013	0.005	0.001
Kidney	NAM M+0	0.808	0.845	0.013	Spleen	NAM M+0	0.780	0.756	0.009
	NAM M+3	0.062	0.053	0.005		NAM M+3	0.159	0.094	0.001
	NAM M+4	0.093	0.068	0.010		NAM M+4	0.047	0.135	0.011
	NAM M+6	0.036	0.033	0.002		NAM M+6	0.015	0.015	0.000
	NAD M+0	0.888	0.940	0.001		NAD M+0	0.806	0.874	0.007
	NAD M+3	0.073	0.041	0.001		NAD M+3	0.182	0.122	0.006
	NAD M+6	0.040	0.019	0.000		NAD M+6	0.012	0.004	0.000
Lung	NAM M+0	0.764	0.782	0.013	Liver	NAM M+0	0.711	0.722	0.017
	NAM M+3	0.074	0.066	0.003		NAM M+3	0.049	0.024	0.002
	NAM M+4	0.146	0.139	0.011		NAM M+4	0.061	0.022	0.018
	NAM M+6	0.017	0.012	0.000		NAM M+6	0.180	0.232	0.002
	NAD M+0	0.878	0.908	0.011		NAD M+0	0.732	0.798	0.009
	NAD M+3	0.115	0.089	0.008		NAD M+3	0.049	0.030	0.001
	NAD M+6	0.007	0.003	0.006		NAD M+6	0.219	0.172	0.010

Table S7. Measured and model-predicted NAD and NAM labeling fractions in tissues, from co-infusion of [U-¹³C]NA and [2,4,5,6-²H]NAM (1:10 ratio, equal to their ratio in serum) for 5 h. Related to Figure 6. Correlation coefficient is 0.997. Measured data are mean ± s.d., n=3.

Tissue	Isotopic fraction	Simulated	Measured		Tissue	Isotopic fraction	Simulated	Measured	
			Mean	s.d.				Mean	s.d.
White Adipose	NAM M+0	0.873	0.877	0.007	Skeletal Muscle	NAM M+0	0.832	0.857	0.000
	NAM M+3	0.061	0.078	0.009		NAM M+3	0.032	0.039	0.003
	NAM M+4	0.057	0.022	0.002		NAM M+4	0.132	0.099	0.007
	NAM M+6	0.009	0.023	0.003		NAM M+6	0.004	0.005	0.004
	NAD M+0	0.925	0.924	0.007		NAD M+0	0.979	0.974	0.007
	NAD M+3	0.065	0.065	0.010		NAD M+3	0.021	0.023	0.003
	NAD M+6	0.009	0.011	0.006		NAD M+6	0.001	0.002	0.003
Brain	NAM M+0	0.850	0.897	0.005	Pancreas	NAM M+0	0.727	0.755	0.009
	NAM M+3	0.058	0.068	0.008		NAM M+3	0.074	0.090	0.008
	NAM M+4	0.088	0.032	0.005		NAM M+4	0.181	0.127	0.009
	NAM M+6	0.004	0.004	0.000		NAM M+6	0.018	0.028	0.000
	NAD M+0	0.937	0.957	0.007		NAD M+0	0.908	0.898	0.003
	NAD M+3	0.061	0.041	0.007		NAD M+3	0.064	0.057	0.000
	NAD M+6	0.002	0.002	0.000		NAD M+6	0.028	0.044	0.003
Heart	NAM M+0	0.890	0.879	0.002	Small Intestine	NAM M+0	0.737	0.743	0.008
	NAM M+3	0.053	0.081	0.002		NAM M+3	0.212	0.202	0.005
	NAM M+4	0.048	0.014	0.003		NAM M+4	0.037	0.033	0.014
	NAM M+6	0.009	0.026	0.001		NAM M+6	0.014	0.022	0.001
	NAD M+0	0.939	0.943	0.000		NAD M+0	0.753	0.776	0.009
	NAD M+3	0.053	0.047	0.002		NAD M+3	0.233	0.209	0.006
	NAD M+6	0.009	0.011	0.001		NAD M+6	0.014	0.016	0.002
Kidney	NAM M+0	0.792	0.783	0.009	Spleen	NAM M+0	0.739	0.781	0.009
	NAM M+3	0.086	0.103	0.002		NAM M+3	0.201	0.185	0.001
	NAM M+4	0.095	0.062	0.001		NAM M+4	0.047	0.015	0.009
	NAM M+6	0.027	0.053	0.005		NAM M+6	0.013	0.018	0.000
	NAD M+0	0.874	0.851	0.002		NAD M+0	0.762	0.825	0.003
	NAD M+3	0.091	0.083	0.001		NAD M+3	0.224	0.160	0.002
	NAD M+6	0.034	0.066	0.001		NAD M+6	0.014	0.015	0.001
Lung	NAM M+0	0.730	0.819	0.006	Liver	NAM M+0	0.867	0.832	0.009
	NAM M+3	0.106	0.129	0.003		NAM M+3	0.066	0.063	0.001
	NAM M+4	0.152	0.030	0.011		NAM M+4	0.061	0.095	0.009
	NAM M+6	0.013	0.022	0.002		NAM M+6	0.006	0.010	0.000
	NAD M+0	0.837	0.876	0.005		NAD M+0	0.934	0.942	0.005
	NAD M+3	0.146	0.110	0.004		NAD M+3	0.061	0.046	0.004
	NAD M+6	0.017	0.014	0.002		NAD M+6	0.005	0.011	0.001

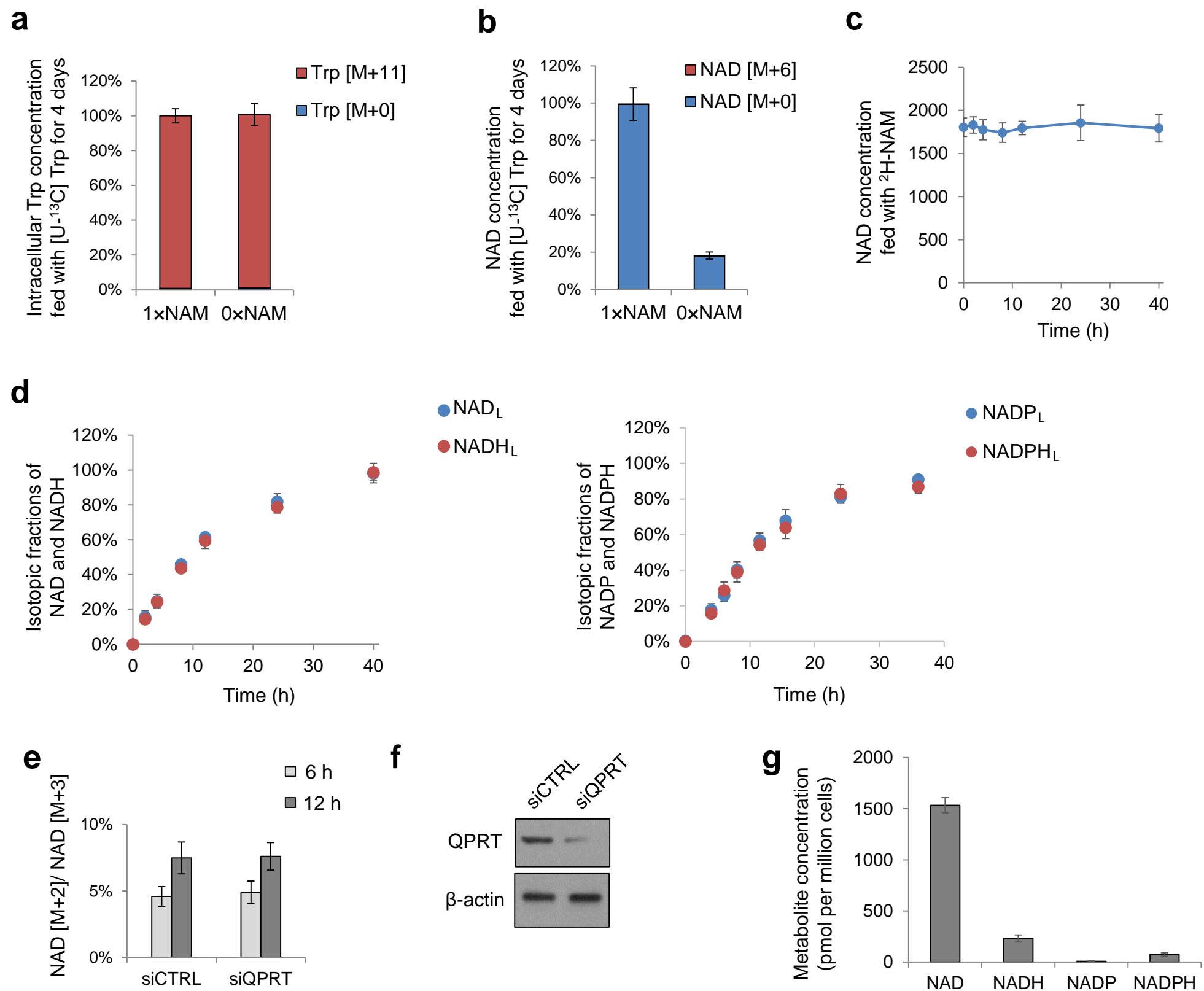


Figure S1. In T47D cells, there is not *de novo* NAD synthesis from tryptophan and NAD M+2 does not arise due to activity of the *de novo* pathway enzyme QPRT. Related to Figure 1 and Figure 2. **(a)** In cells grown in [U-¹³C] Trp in normal DMEM (1x NAM) or NAM-free DMEM (0x NAM) for 4 days, intracellular tryptophan is essentially fully labeled. **(b)** NAD is not detectably labeled. Absolute signal intensity for Trp and NAD are normalized to the signal in standard DMEM. **(c)** NAD concentration in cells fed ²H-NAM. **(d)** Indistinguishable labeling of NAD and NADH (left) and NADP and NADPH (right) in cells fed ²H-NAM. **(e)** Knockdown of QPRT does not alter the ratio between NAD [M+2] and NAD [M+3] following 6 h or 12 h of ²H-NAM labeling. **(f)** Western blot for QPRT knockdown. **(g)** Concentrations of NAD, NADH, NADP and NADPH. Data are mean \pm s.d., n = 3.

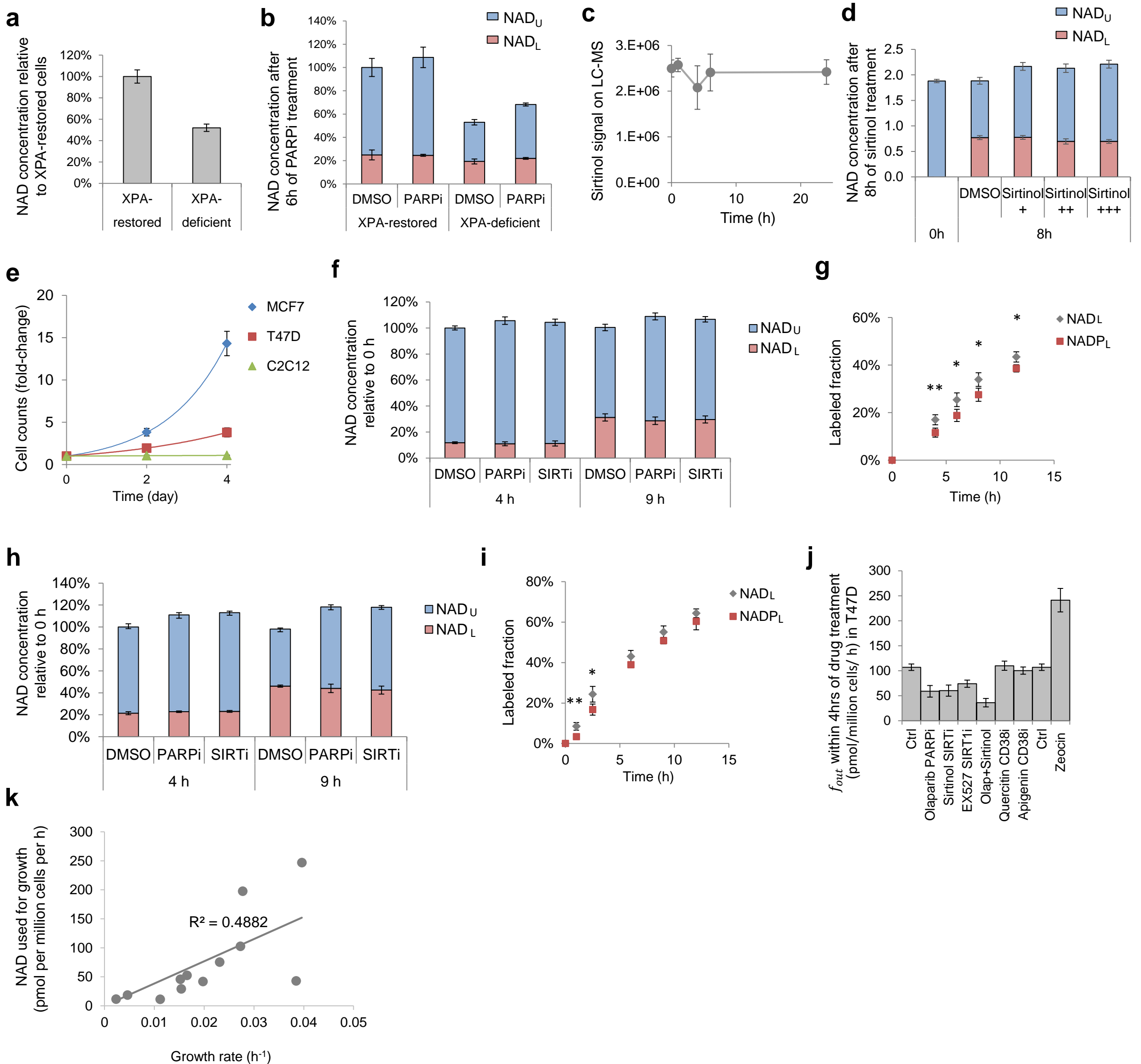


Figure S2. Role of growth, PARP, sirtuins, and CD38 in NAD turnover in selected cell types. Related to Figure 3. **(a)** NAD concentration in XPA-deficient or XPA-restored cells (relative to restored cells). **(b)** NAD concentration and labeling in XPA-deficient and XPA-restored cells treated with DMSO (negative control) or olaparib (10 μ M, PARP1/2 inhibitor) for 6 h. Olaparib was added simultaneously with switching cells into ²H-NAM. **(c)** Stability of 50 μ M sirtinol in DMEM supplemented with 10% DFBS (37° C). **(d)** NAD concentration and labeling in T47D cells treated with DMSO (negative control), 25 μ M sirtinol (+), 50 μ M sirtinol (++), or 100 μ M sirtinol (+++), for 8 h. Sirtinol was added simultaneously with switching cells into ²H-NAM. **(e)** Growth rate of MCF7, T47D and differentiating C2C12 cells. Lines are single exponential fits. **(f)** Measurement of NAD consumption by PARPs and sirtuins in MCF7 cells. NAD concentration and labeling was measured in cells treated with DMSO, olaparib (10 μ M), or sirtinol (25 μ M) for 4 h or 9 h. Drug was added simultaneously with switching cells into ²H-NAM. **(g)** Measurement of NAD consumption by NAD kinase in MCF7 cells. Cells were fed ²H-NAM starting at t = 0 and NAD and NADP labeling were measured. NAD labeling significantly exceeded NADP labeling at early time points (**p<0.01, * p<0.05, paired t-test). **(h, i)** Same as (f, g) but in C2C12 cells. For panel a-i, data are mean \pm s.d., n = 3. **(j)** CD38 does not consume substantial NAD in T47D cells. Consumption rates were calculated based on 4 h incubation with ²H-NAM and quercetin (50 μ M, CD38 inhibitor) or apigenin (25 μ M, CD38 inhibitor). Bars are mean \pm 95% confidence interval of f_{out} . **(k)** Across the same 12 cell lines as Figure 4, NAD usage for growth correlates with growth rate (p=0.01).

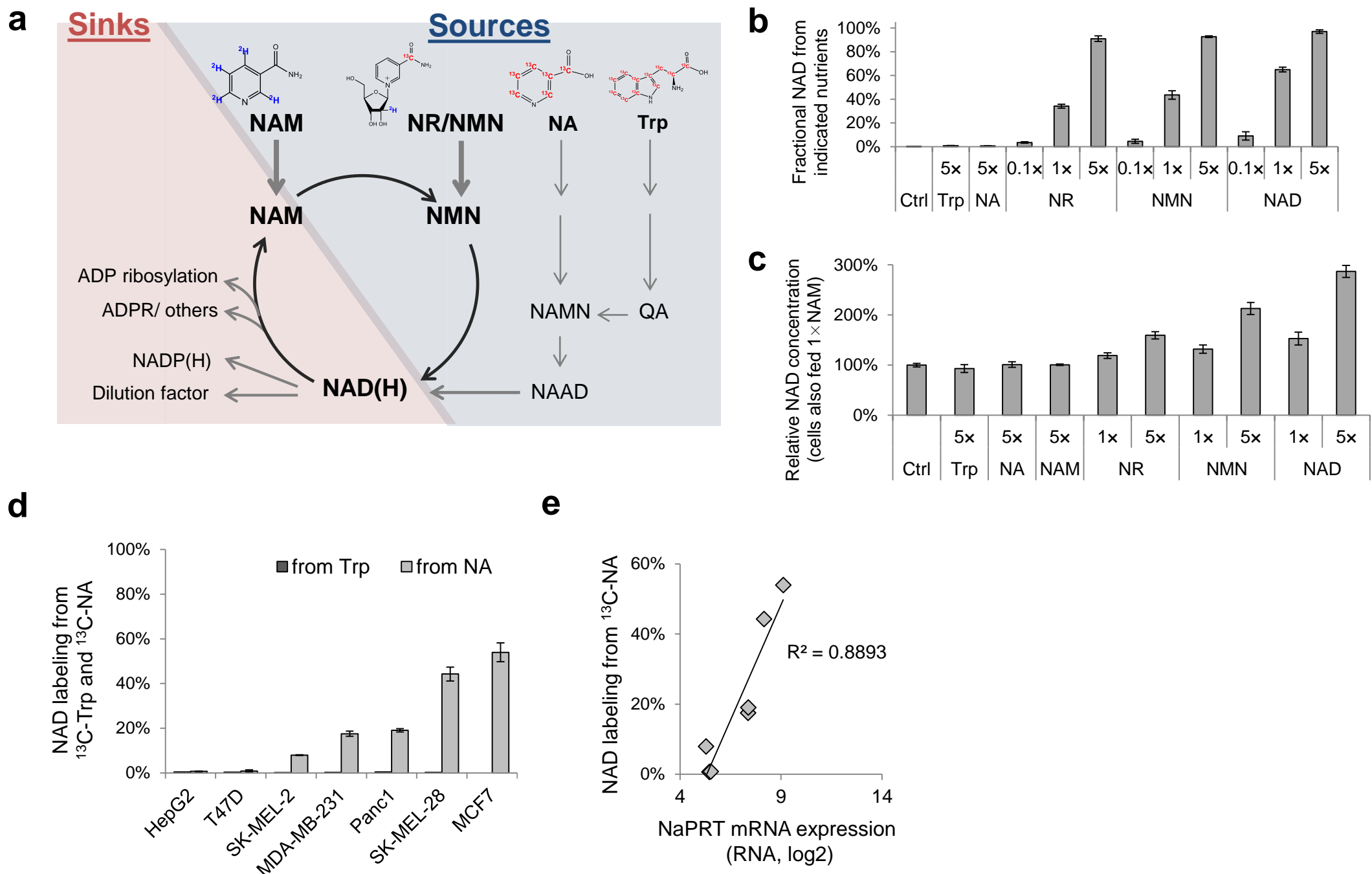


Figure S3. Contributors to NAD biosynthesis in cell lines. Related to Figure 5. **(a)** NAD biosynthesis and consumption schematic. Trp, Tryptophan; NA, nicotinic acid; NR, nicotinamide riboside; NAM, nicotinamide; NMN, nicotinamide ribotide; QA, quinolinic acid; NAAD, nicotinic acid adenine dinucleotide. **(b)** Fraction of NAD in T47D cells coming from the indicated supplemented substrate based on isotope tracing for 24 h. Compound concentrations are reported relative to nicotinamide in commercial DMEM (32 μ M NAM = 1x). **(c)** NAD concentration in T47D cells fed DMEM supplemented with additional precursors for 48 h. **(d)** Labeling fraction of NAD in cells fed [U- 13 C]Trp (5x) or [U- 13 C]NA (1x) in DMEM for 48 h. Data are mean \pm s.d., n = 3. **(e)** Across cell lines, the fraction of NAD coming from NA (data from panel d) correlates with NaPRT1 mRNA expression (data from <https://portals.broadinstitute.org/ccle/>).

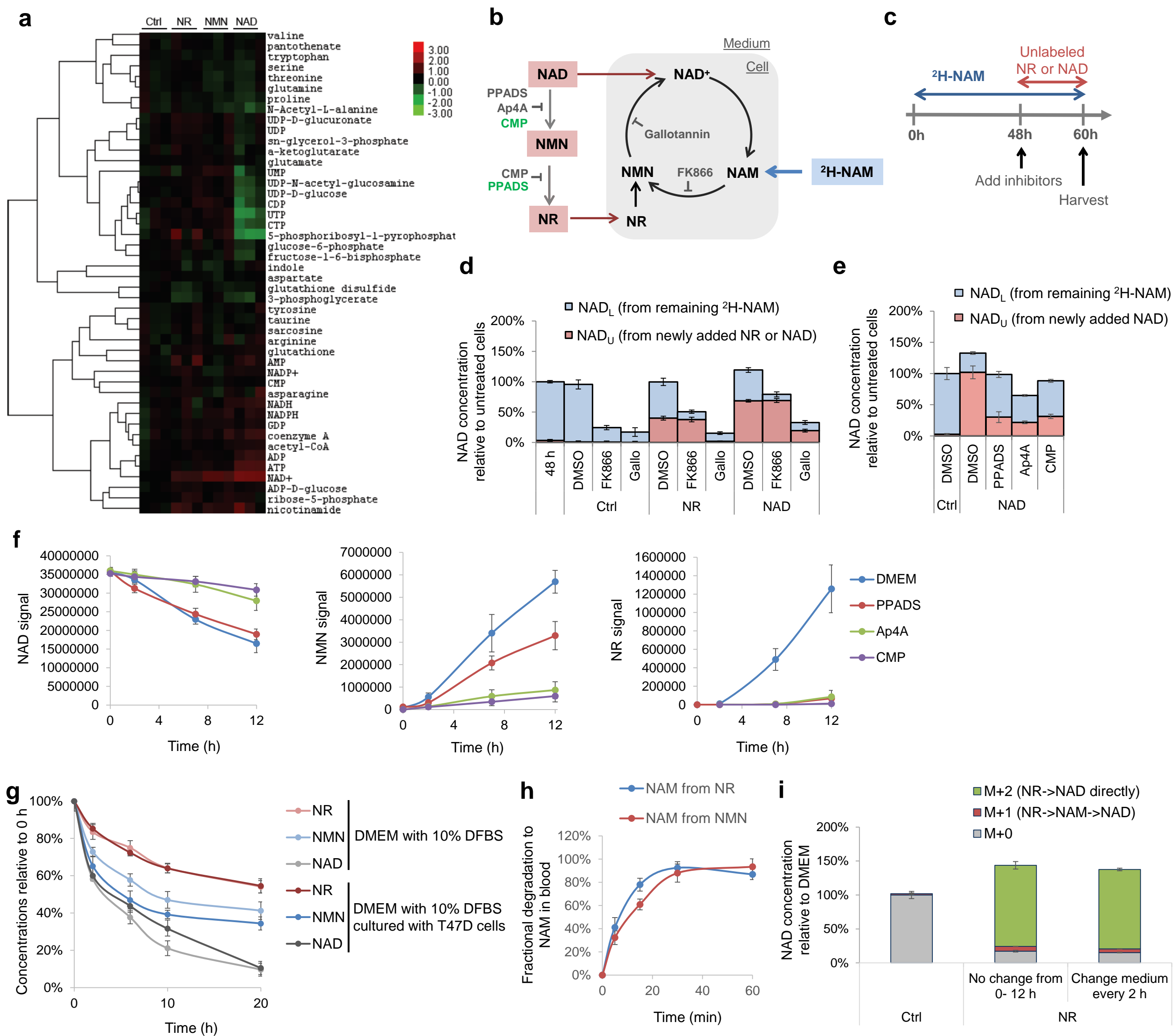


Figure S4. Metabolic impact and assimilation routes of NR, NMN, and NAD. Related to Figure 5 and Figure 7. **(a)** Heat map of metabolite concentration changes in T47D cells in response to NR, NMN, NAD (5x the concentration of NAM, individually in the presence of NAM) after 24 h. Each column represents one sample. Data were normalized to cell number. All individual samples were then normalized to the average of the control (DMEM) samples. **(b)** Schematic illustrating (i) the intracellular steps at which of gallotannin (Gallo, NMNAT inhibitor) and FK866 (NAMPT inhibitor) target NAD metabolism, (ii) the extracellular step at which Ap4A blocks the degradation of NAD to NMN, and (iii) the extracellular steps at which PPADS and CMP are expected based on literature to act (grey³⁸) or were detected to act in this study (green). **(c)** Experimental design to test pathway steps required for assimilation of NR and NAD. Cells were fed ²H-NAM for 48 h, after which unlabeled precursors (NAD or NR, 1x) and inhibitors (100 nM FK866, 100 μM gallotannin, 25 μM PPADS, 1 mM Ap4A or 2 mM CMP) were simultaneously added for 12 h. **(d)** NAD concentration and labeling in T47D cells with 12 h FK866 or gallotannin treatment. Newly added NR bypassed FK866 but was blocked by gallotannin, while newly added NAD was taken intact partially and thus bypassed both steps. **(e)** NAD concentration and labeling in T47D cells treated for 12 h with PPADS, Ap4A, or CMP. Blockade of NAD degradation by these inhibitors (as verified in panel f) partially but not fully blocked assimilation of extracellular NAD into intracellular NAD, suggesting that extracellular NAD can contribute to the intracellular NAD pool both by direct uptake and by extracellular degradation to NR followed by cellular NR uptake and metabolism. Because PPADS, Ap4A, or CMP treatment reduced unlabeled NAD by ~80%, it is likely that only a minor fraction of extracellular NAD is directly taken up by the cell, with most NAD entering the cell after its extracellular degradation. **(f)** Degradation of NAD (300 μM) into NMN and NR in fresh DMEM supplemented with 10% DFBS at 37 ° C, and its inhibition by PPADS, Ap4A or CMP (at the above concentrations). Unexpectedly, CMP prevented degradation of NAD to NMN, rather than exclusively blocking NMN to NR, and PPADS only modestly blocked degradation to NMN, despite preventing the appearance of NR. **(g)** Stability of 100 μM NR, NMN and NAD in DMEM supplemented with 10% DFBS (37 ° C), and in DMEM with 10% DFBS cultured with T47D cells. Concentrations were normalized to 0 h. **(h)** Degradation of NR and NMN into NAM in blood at 37 ° C. NAM concentrations were normalized to the added NR and NMN concentration (100 μM). **(i)** NAD concentration in T47D cells fed ²H,¹³C-NR (5x, 32 μM=1x) for 12 h. Medium was either refreshed every 2 h, or remained unchanged. Data are mean ± s.d., n = 3. Lines are to guide the eye.

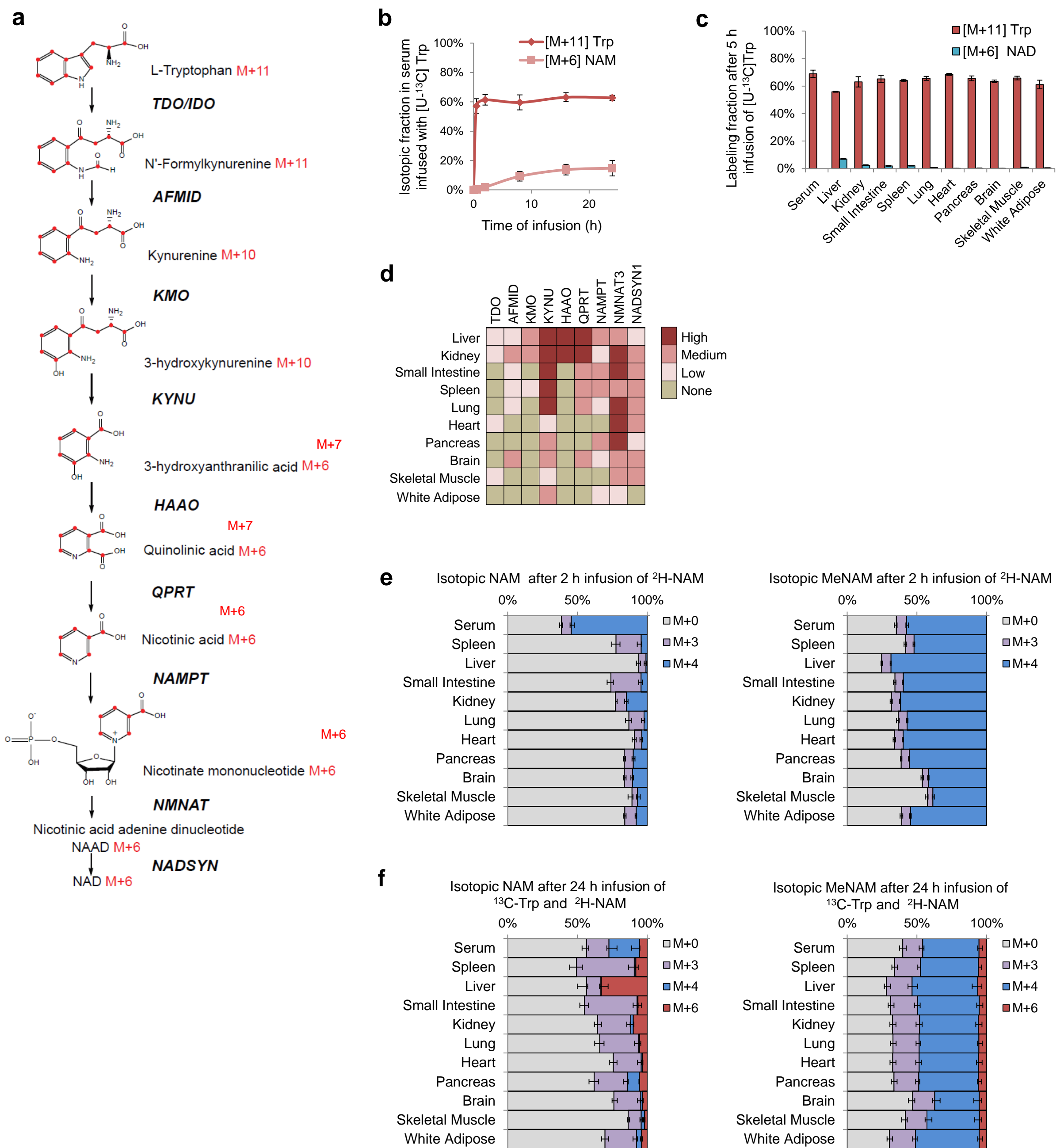


Figure S5. *De novo* NAD synthesis, and labeling of NAM and N-methylnicotinamide (MeNAM). Related to Figure 5. **(a)** *De novo* pathway with labeling states of intermediates from [U-¹³C]Trp indicated. **(b)** Isotopic fractions of tryptophan and NAM in serum. ¹³C-Trp was infused via jugular vein at 5 nmol/g/min. Lines are to guide the eye. **(c)** Labeled fractions of tryptophan and NAD in tissues after 5 h [U-¹³C]Trp infusion. Note that NAD labeling is greatest in liver. Data are mean \pm s.d., n=3. **(d)** Liver and kidney have the complete set of NAD *de novo* synthesis enzymes. Data are from the Human Protein Atlas. **(e-f)** NAM and MeNAM labeling in serum and tissues. MeNAM displayed similar labeling across tissues, indicating rapid sharing of MeNAM (unlike NAM itself) throughout the body via the circulation. Mice were either infused with ²H-NAM for 2 h **(e)**, or co-infused with ²H-NAM and ¹³C-Trp for 24 h **(f)**. Data are mean \pm s.d., n=2.

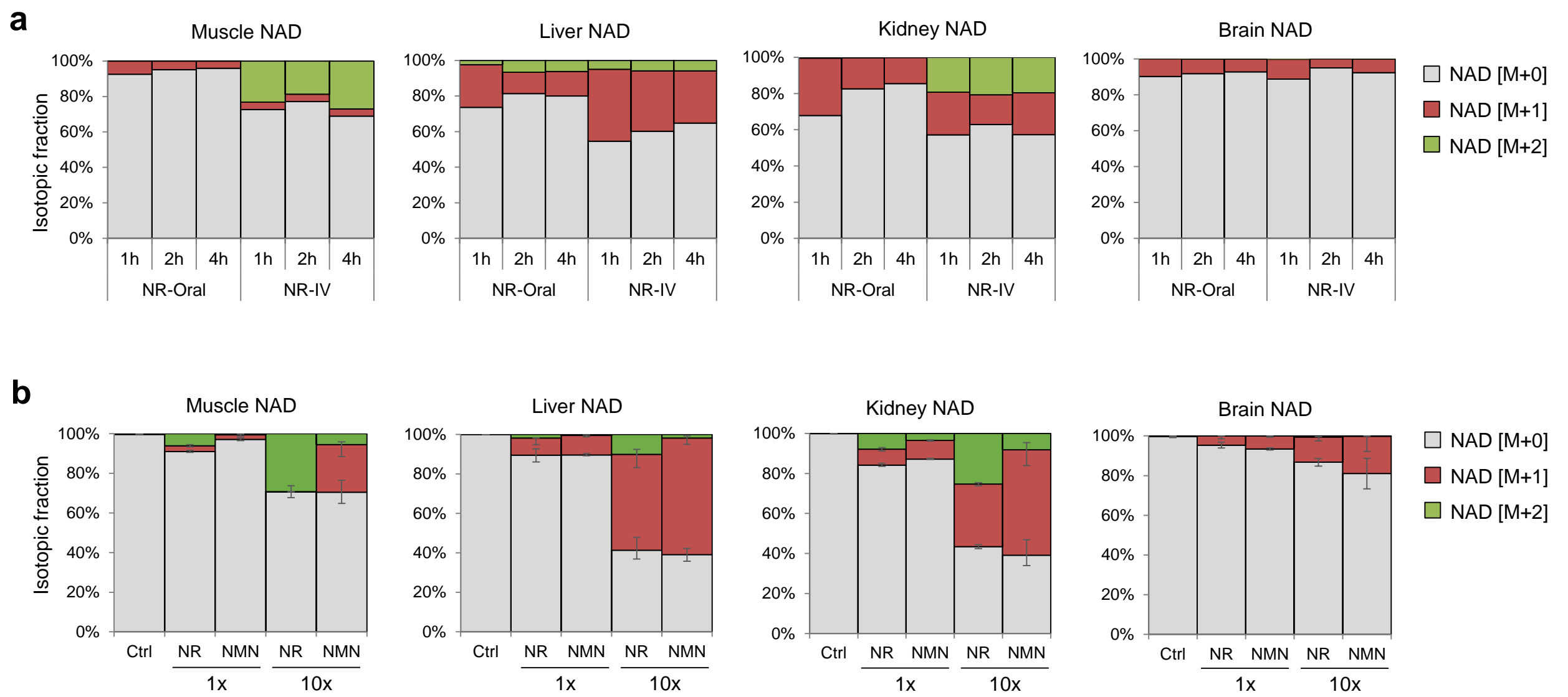


Figure S7. Metabolism of high dose NR and NMN. Related to Figure 7. **(a)** Tissue NAD labeling, at the indicated times after a 200 mg/kg bolus (4x) of $^2\text{H}, ^{13}\text{C}$ -NR by oral gavage or by IV injection ($n=1$ per time point). **(b)** Tissue NAD labeling after 2 h of either 50 mg/kg (1x) or 500 mg/kg (10x) bolus of $^2\text{H}, ^{13}\text{C}$ -NR or $^2\text{H}, ^{13}\text{C}$ -NMN by IV injection. Data are mean \pm s.d., $n=3$ for 50 mg/kg (1x), $n=5$ for 500 mg/kg (10x).